US-TEC
Validation

Prepared by:
Tim Fuller-Rowell, Doug Robertson, Abe Jacobson, Eduardo Araujo-Pradere, Cliff Minter, and Mihail Codrescu

Space Environment Center and National Geodetic Survey
US-TEC
Last modified:10/21/05

Introduction

This document described the current status of the on-going validation of US-TEC. Validation of absolute TEC is a challenge because there are very few direct TEC measurements that are "unbiased." One of the key components of a good metric is to have a reliable and accurate measurement against which to compare the model. The accuracy of the US-TEC map is expected to be in the range of 1 to 3 TEC units, so ideally the measurement requirement for the metric should be accurate to less than 1 TEC unit, in order for the validation to be meaningful. Ionosondes provide an estimate of TEC but it is not sufficiently accurate since there is no topside data to estimate the thickness of the electron density profile. Data from the TOPEX/Poseidon and Jason satellite would be preferable, but the data are only available over the oceans where no CORS station exists, and there is a bias in the data that has to be estimated.

Because of the difficulty in obtaining an absolute unbiased TEC measurement, part of the validation effort is devoted to a differential accuracy estimate. The differential method is internal, but may reflect the absolute accuracy in some cases. The absolute method utilizes data from the Los Alamos Fast Onboard Recording of Transient Events (FORTE) satellite (Moses and Jacobson, 2004). The FORTE satellite at 800 km altitude includes a broadband RF receiver between 30-300 MHz. By recording the transmission from a simulated lightning pulse, the time delay as a function of frequency can be used to estimate the absolute TEC along the transmission path from transmitter to the satellite.

In addition to describing the analysis of both a differential and absolute TEC, this validation document also provides an assessment of the reliability of the CORS data feed. The validation therefore covers three areas:

1. **Reliability of CORS GPS real-time data feed**
2. **Analysis of Differential TEC**
3. **Analysis of Absolute TEC**

1. **Reliability of CORS GPS real-time data feed**.

The CORS data feed from the US Coast Guard dual-frequency GPS receivers began to be transmitted to SEC in real-time in April 2004, via for CORS-West data collector in the National Geophysical Data Center (NGDC). Since that time the reliability of the data feed has been evaluated. **Figure 1** shows a time history of the number of GPS sites that were available in real-time for every 15-minute cycle of the US-TEC process. Apart from the three periods when the data dropouts occurred, just less than 60 stations were available throughout the 6-month period. The data disruptions resulted from changes in computer configuration at the CORS-West collector or the processor running US-TEC within SEC. Overall there is about 90% reliability, during this initial period. Reliability is expected to improve now the system has been established.

In an effort to further improve reliability and robustness of the product, a parallel data feed is being established from the twin receiver from each of the US Coast Guard sites.

With the added redundancy of the dual feed and the reliability is expected to increase to close to 99%. The accuracy of the TEC specification is also expected to improve as the number of stations gradually rises.
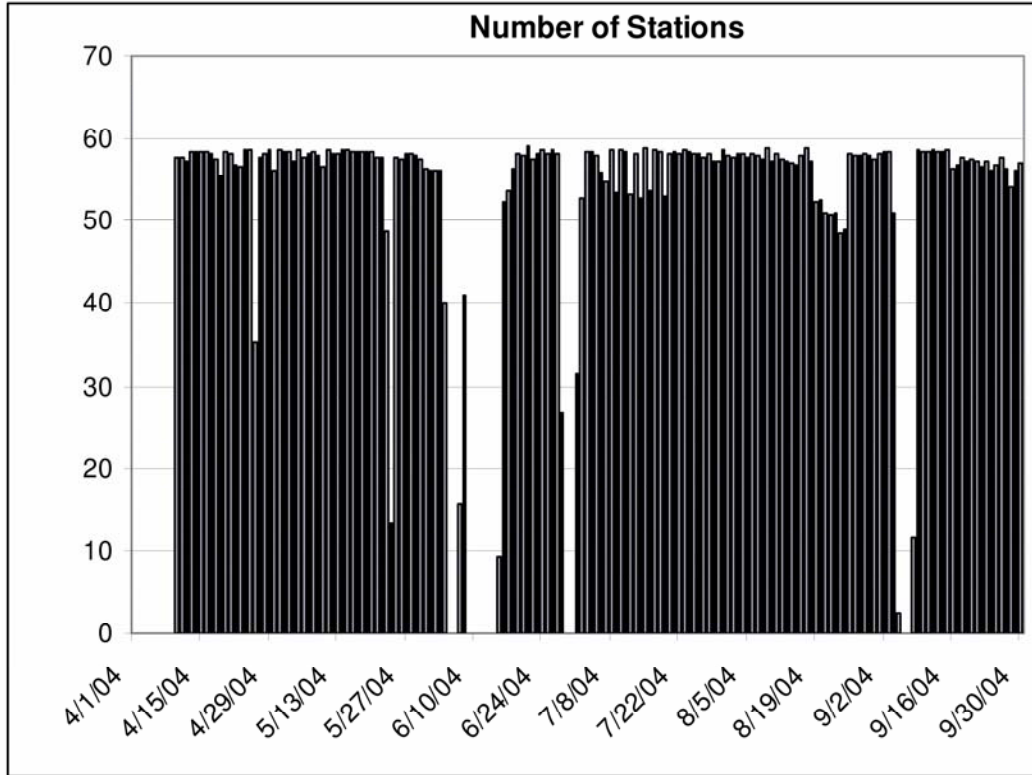

Figure 1: Time series of the number of GPS stations that were available in real-time for the USTEC process.

2. **Analysis of Differential TEC**

If continuous GPS data are available along a given receiver–satellite link with no cycle slips, estimates of the phase difference (scaled to TEC units) from one epoch to the next can be determined with an accuracy of less than 0.1 TEC units. This fact can be utilized to estimate the uncertainty in the US-TEC vertical and slant path maps. By integrating through US-TEC inversion maps at two different times, the difference in the slant TEC can be compared with the direct phase difference in the original RINEX data file.

The method computes the phase differences between two rays separated in time for a particular satellite and receiver pair. As the time difference between the rays tends to zero, the TEC difference will tend to zero and the error as compared to the inversion will tend to zero. Increasing the time difference between the rays, the phase differences will increase and the inversion error along each ray will decorrelate (see below).

TEC difference measured from RINEX at two times t_a and t_b is given by:

$$P(t_a)-P(t_b)) \hspace{4cm} (1)$$

TEC difference from inversion, $I(t)$, subject to error e

$$(I(t_a)+e(t_a)) - (I(t_b)+e(t_b))$$

$$=(I(t_a)-I(t_b)) + (e(t_a)-e(t_b)) \hspace{3cm} (2)$$

For small times differences t_a-t_b, $e(t_a)$ and $e(t_b)$ will correlate (i.e. the ionosphere may be systematically low for both rays) hence the errors will cancel. However, for a sufficiently large time difference the errors should decorrelate, so the error estimate will tend to saturate to the actual error in the US-TEC inversion. The differential accuracy analysis computes a Root Mean Square Error (RMSE) between the RINEX TEC difference and inversion TEC differences for paths between a given receiver and all satellites over the whole day. **Figure 2** shows an example for the WHN1 receiver at Whitney, Nebraska. The figure shows the gradual increase in the RMSE as the time difference between the rays increases. The value tends to plateau, or saturate, at about 2 TEC units. The RMSE for the International Reference Ionosphere (IRI) is also shown, which has a consistently larger error and does not reach a plateau. Note that the RMSE for this study is representative of the uncertainty in the average slant path TEC. The equivalent error for vertical TEC is expected to be about a factor of about 1.3 lower, depending on the average elevation angle of all the satellites in view.
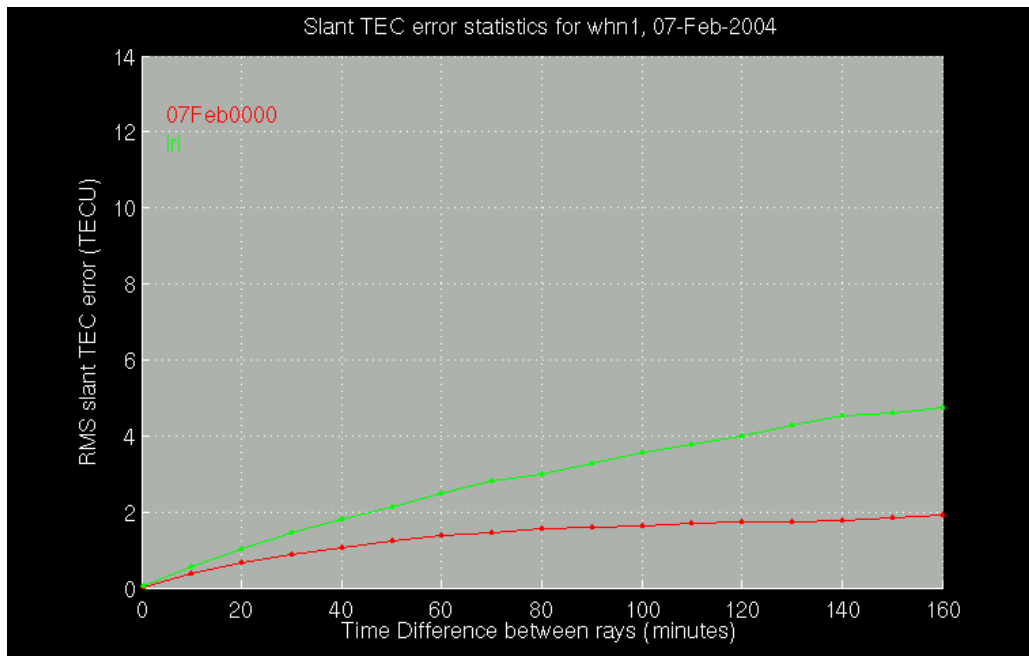

Figure 2: Example of the differential TEC validation

The final error estimate (from the saturation level) will be an averaged estimate for the day. If no saturation occurs (as it is common with the IRI) it implies that values are

systematically biased over length scales greater than a few hours, so cannot be estimated with this method.

The estimates of accuracy using the differential method have been performed for nine stations spread over the CONUS; the data for none of these sites were included in the assimilation process. At each station the daily averaged RMSE analysis has been performed every fifth day since March 2004. The stations chosen are:

PABH: Florida Beach, Washington,

YBHB: Yreka, California

BILL: Lake Skinner, California

CLK1: Clark 1, South Dakota

HBRK: Hillsboro, Kansas

ARP3: Aransas Pass 3, Texas

WES2: Haystack Observatory, Westford, Massachusetts

VIMS: Virginia Institute of Marine Science, Wachapreague, Virginia

CCV3: Cape Canaveral 3, Florida

For each site, the daily average RMSE of the differential TEC has been evaluated for every fifth day between April and September. Table 1 shows the RMSE statistics at a time difference of 160 minutes, for each station and day, and the averages over the 6 month period. The values from the IRI are also shown. Note that in most cases the RMSE for IRI has not reached a plateau, so the values sampled at a time difference of 160 minutes (see example in Figure 2) are not expected to reflect the true uncertainty. For each day the average number of stations available for the 96 TEC maps during that day is displayed, together with the RMSE difference between US-TEC and IRI and the daily A_p. Note that on days where no data are available, the US-TEC RMSE is close to IRI, as expected. On typical days when about 60 stations are consistently available, the uncertainty for the slant path TEC is between 2 and 3 TEC units. The average RMSE for all conditions over the 6-month period is 2.4 TEC units , which is equivalent to just less than 2 TEC units uncertainty in the vertical TEC. Note that on the storm day, July 25 2005, the RMSE rises slightly to 3.3 TEC units, which is expected due to the steeper gradients existing during geomagnetic storms.

Table 1 (Apr–Jun)

	Apr						May						Jun					
IRI	5	10	15	20	25	30	5	10	15	20	25	30	5	10	15	20	25	30
pabh		3.8	3.4	2.4	3.6		2.7	3.0	2.7	6.4	4.4	3.1		2.4		3.3	5.3	1.8
ybhb		4.1	3.2	3.0	3.7		3.3	3.2	2.8	7.3	5.3	4.0		3.5		4.2	5.1	2.9
bill		4.8	4.9	3.5	4.1		6.2	3.7	4.3	9.2	5.1	5.1		5.2		5.1	6.2	3.2
clk1		3.2	4.5	2.7	4.4		3.8	3.8	3.1	6.2	5.5	3.3		2.3		3.9	5.3	2.4
hbrk		4.6	5.1	2.9	4.1		4.1	4.7	3.6	7.8	4.9	4.2		3.2		4.4	5.9	3.9
arp3		4.6	7.8	3.8	5.1		5.2	4.6	5.4	7.2	4.1	4.9		4.8		4.5	5.9	4.2
wes2		3.7	4.0	3.7	4.0		3.1	4.5	2.9	5.8	3.4	3.9		2.7		3.0	4.5	3.3
vims		4.3	4.6	2.6	4.2		4.2	4.6	3.1	6.8	4.6	4.2		3.1		3.4	5.6	4.4
ccv3		4.5		2.6	5.0		5.3	4.2	4.5	5.1	3.8	4.6		3.8		4.2	5.5	6.9
AVE		4.2	4.7	3.0	4.2		4.2	4.0	3.6	6.9	4.6	4.1		3.5		4.0	5.5	3.7
USTEC																		
pabh		1.7	1.7	1.6	1.9		1.6	1.8	1.9	3.3	2.0	1.6		2.4		1.7	2.1	1.8
ybhb		2.0	1.6	1.8	2.3		2.1	2.0	2.2	3.4	2.5	2.0		3.5		2.5	2.4	2.8
bill		2.4	2.4	2.4	2.5		2.7	2.7	3.1	5.1	2.8	3.0		5.2		3.0	3.5	3.1
clk1		1.5	1.8	1.5	1.8		1.5	1.8	1.6	2.3	1.9	1.7		2.3		2.0	2.5	2.5
hbrk		1.8	1.7	1.5	1.8		2.2	2.1	1.6	2.5	2.3	1.6		3.2		1.7	2.4	3.8
arp3		2.4	3.4	3.5	2.5		2.7	2.8	3.4	4.1	2.7	3.4		4.8		3.0	3.7	4.2
wes2		1.8	1.5	1.6	1.4		1.7	2.2	1.8	2.8	1.6	1.6		2.8		2.0	2.0	3.3
vims		1.7	1.7	1.4	1.6		1.8	2.1	1.7	2.5	2.0	1.3		3.1		1.6	2.1	4.4
ccv3		2.5		2.6	2.9		2.9	2.3	2.1	2.7	2.2	2.2		3.9		2.4	2.4	6.9
AVE		2.0	2.0	2.0	2.1		2.1	2.2	2.2	3.2	2.2	2.0		3.5		2.2	2.6	3.6
USTEC - IRI																		
pabh		-2.1	-1.6	-0.8	-1.7		-1.1	-1.2	-0.8	-3.1	-2.4	-1.5		0.0		-1.6	-3.2	0.0
ybhb		-2.2	-1.6	-1.2	-1.3		-1.2	-1.2	-0.6	-3.9	-2.8	-2.0		0.0		-1.7	-2.6	-0.1
bill		-2.4	-2.6	-1.1	-1.6		-3.5	-1.1	-1.2	-4.1	-2.3	-2.1		0.0		-2.1	-2.7	-0.1
clk1		-1.7	-2.7	-1.2	-2.6		-2.3	-2.0	-1.5	-3.9	-3.6	-1.6		0.0		-1.9	-2.8	0.0
hbrk		-2.8	-3.4	-1.4	-2.3		-2.0	-2.6	-2.0	-5.3	-2.6	-2.6		0.0		-2.6	-3.5	0.0
arp3		-2.2	-4.4	-0.4	-3.1		-2.4	-1.7	-2.0	-3.1	-1.4	-1.5		0.0		-1.6	-2.2	0.0
wes2		-1.9	-2.6	-2.1	-2.6		-1.4	-2.2	-1.1	-3.0	-1.8	-2.3		0.0		-1.1	-2.5	0.0
vims		-2.6	-2.9	-1.2	-2.7		-2.3	-2.6	-1.4	-4.3	-2.6	-3.0		0.0		-1.7	-3.5	0.0
ccv3		-2.0			-2.1		-2.4	-1.9	-2.4	-2.4	-1.6	-2.4		0.1		-1.8	-3.1	0.1
AVE DIF		-2.2	-2.7	-1.0	-2.2		-2.1	-1.8	-1.4	-3.7	-2.3	-2.1		0.0		-1.8	-2.9	0.0
ap index	14	10	6	4	12	12	13	7	9	13	8	13	11	11	16	3	4	10
# stations		58	58	58	59	56	59	57	59	58	58	57	0	0	9	58	58	0

Table 1 (Jul–Sep)

	Jul						Aug						Sep						AVE
IRI	5	10	15	20	25	30	5	10	15	20	25	30	5	10	15	20	25	30	
pabh	2.6	4.1	4.4	3.2	6.1	1.6	2.6	2.0	4.5	3.9	4.0	2.8		4.2	2.1	2.0	3.0	2.9	3.4
ybhb	3.4	4.5	4.6	4.0	7.3	2.8	2.9	3.8	4.5	4.5	3.9	4.2		4.4	3.3	3.0	4.1	4.1	4.0
bill	5.0	5.0	5.4	5.2	7.8	3.3	4.0	5.2	4.5	4.0	4.2	4.6		3.5	3.8	9.7	4.9	6.4	5.1
clk1	2.3	2.4	5.5	4.3	6.9	2.6	3.0	2.9	4.1	3.9	4.2	4.5		5.0	4.7	2.1	2.5	3.1	3.8
hbrk	3.7	3.6	6.0	4.7	9.5	3.5	3.6	3.1	5.3	3.4	3.2	3.5		4.7	4.9	2.8	4.0	3.4	4.4
arp3	4.9	5.1	5.1	5.3	8.1	3.3	3.6	4.6	4.9	4.1	3.2	6.9		4.2	4.7	3.7	5.7	5.0	5.0
wes2	2.9	4.0	4.9	5.0	6.7	3.0	3.0	3.4	5.8	3.7	2.9	4.8		4.8	4.2	2.7	2.3	2.5	3.8
vims	3.5	4.9	5.8	4.8	8.6	4.0	2.9	3.5	6.0	2.6	3.3	4.7		3.1	5.3	2.8	3.6	2.9	4.3
ccv3		5.9	6.2	5.1	7.6	3.6	3.2	3.2	6.3	3.4		4.3		3.1	4.3	2.8	4.2	3.1	4.5
AVE	3.5	4.4	5.3	4.6	7.6	3.1	3.2	3.5	5.1	3.7	3.6	4.5		4.1	4.2	3.5	3.8	3.7	4.2
USTEC																			
pabh	1.9	1.9	1.8	1.6	3.2	1.1	1.6	1.2	2.0	2.0	1.9	1.8		1.7	1.3	1.6	1.7	1.7	1.9
ybhb	2.0	2.8	2.3	2.1	2.9	1.7	1.9	1.6	2.5	2.6	2.5	2.3		2.2	2.1	1.8	2.1	2.5	2.3
bill	3.1	3.5	3.4	3.5	3.7	2.1	2.5	2.4	3.0	2.8	2.3	2.9		2.7	2.6	8.9	2.7	3.5	3.2
clk1	1.6	1.5	2.1	2.5	3.2	1.3	1.6	1.9	1.8	2.1	2.4	2.9		2.2	2.4	1.2	1.3	1.5	1.9
hbrk	1.9	1.6	2.2	2.6	3.9	1.5	1.7	1.7	2.1	2.1	2.3	2.0		2.0	2.3	1.3	1.6	1.9	2.1
arp3	3.4	2.8	2.8	3.9	2.8	1.9	2.7	2.6	3.0	3.5	1.8	4.7		3.3	3.3	2.3	2.9	3.3	3.2
wes2	1.7	1.9	2.2	1.8	2.9	1.4	1.6	1.9	2.6	1.3	1.8	2.4		2.3	2.3	1.5	1.4	1.6	2.0
vims	1.9	1.7	2.1	2.0	4.0	1.5	1.8	1.9	2.4	1.6	2.3	2.3		2.0	2.5	1.7	1.5	1.4	2.0
ccv3		2.8	2.4	3.0	3.1	1.6	2.0	2.2	2.8	2.4		2.4		2.4	2.6	2.1	2.3	2.3	2.7
AVE	2.2	2.3	2.4	2.5	3.3	1.6	1.9	1.9	2.5	2.3	2.2	2.6		2.3	2.4	2.5	2.0	2.2	2.4
USTEC - IRI																			
pabh	-0.8	-2.2	-2.5	-1.5	-2.9	-0.4	-1.1	-0.8	-2.5	-1.9	-2.1	-1.0		-2.5	-0.8	-0.4	-1.3	-1.2	-1.5
ybhb	-1.4	-1.7	-2.4	-1.9	-4.4	-1.1	-1.0	-2.2	-2.0	-1.9	-1.3	-1.9		-2.1	-1.3	-1.2	-2.0	-1.6	-1.7
bill	-1.9	-1.6	-2.0	-1.7	-4.0	-1.2	-1.5	-2.8	-1.5	-1.2	-1.9	-1.7		-0.9	-1.2	-0.8	-2.3	-3.0	-1.9
clk1	-0.7	-0.9	-3.4	-1.8	-3.7	-1.3	-1.4	-1.0	-2.4	-1.8	-1.8	-1.5		-2.8	-2.3	-0.9	-1.2	-1.7	-1.9
hbrk	-1.9	-2.0	-3.8	-2.1	-5.6	-2.0	-1.9	-1.3	-3.2	-1.4	-0.8	-1.5		-2.7	-2.6	-1.5	-2.4	-1.5	-2.3
arp3	-1.5	-2.3	-2.3	-1.5	-5.3	-1.4	-1.0	-2.0	-1.8	-0.6	-1.4	-2.2		-1.0	-1.4	-1.4	-2.8	-1.7	-1.8
wes2	-1.2	-2.1	-2.7	-3.2	-3.7	-1.6	-1.4	-1.5	-3.2	-2.3	-1.0	-2.3		-2.6	-1.9	-1.1	-0.9	-0.9	-1.9
vims	-1.6	-3.3	-3.7	-2.8	-4.5	-2.5	-1.1	-1.6	-3.6	-1.1	-1.0	-2.4		-1.2	-2.8	-1.1	-2.1	-1.5	-2.2
ccv3		-3.0	-3.8	-2.1	-4.5	-2.0	-1.2	-0.9	-3.5	-1.0		-1.9		-0.7	-1.7	-0.7	-1.8	-0.8	-1.8
AVE DIF	-1.4	-2.1	-3.0	-2.1	-4.3	-1.5	-1.3	-1.6	-2.6	-1.4	-1.4	-1.8		-1.8	-1.8	-1.0	-1.9	-1.5	-1.9
ap index	7	8	9	9	122	7	7	14	7	14	7	34	7	5	14	13	5	4	
# stations	58	59	59	58	58	57	58	57	57	53	49	58	3	58	59	58	57	57	50

Table 1: RMSE of differential TEC for IRI and US-TEC for each of nine reference stations between April and September 2005.

3. Analysis of Absolute TEC

The purpose of the absolute validation is to confirm, or otherwise, the notion that the differential TEC validation, described above, provides a realistic estimate of the slant path TEC uncertainty. This analysis requires measurements of TEC that are accurate to less than 1 TEC units. None of the conventional data sources, including ionosondes, TOPEX, and dual frequency GPS, reach this criteria due to a variety of reasons. Possible sources of data with sufficient accuracy are satellite based lightning detectors. There are two satellite-based VHF lightning detection projects at Los Alamos (DOE), the FORTE (Fast On-Orbit Recording of Transient Events) system and the V-GLASS (VHF Global Lightning and Severe Storm monitor) system. We have performed an analysis comparing the FORTE data with US-TEC. In a later study we hope to obtain data from the experimental version of the V-GLASS system on-board the Block IIR GPS constellation. This data is currently classified.

FORTE was launched in 1997 and consists of a suite of VHF lightning receivers, an optical CCD imager and an optical photodiode. The VHF receivers ceased operation in 2001 and the optical instruments continue to operate. The FORTE data is completely unclassified. **Figure 3** shows an example of the FORTE data.
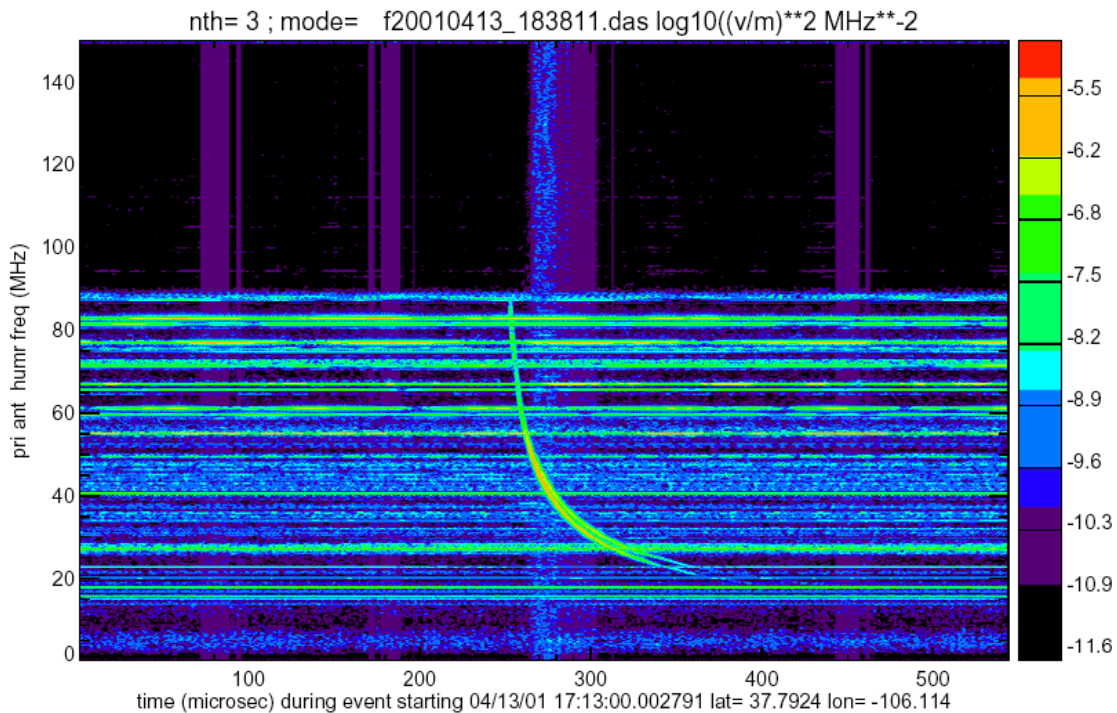

Figure 3: Example of the observation of the signal delay as a function of frequency from the FORTE satellite.

With the FORTE broadband signal, the phase can unambiguously be connected across a wide bandwidth, and the problem of resolving the phase ambiguity in different channels does not arise. The $1/f^2$ curve fit to this data, and the resulting coefficient provides the unambiguously TEC in some appropriate units. Note that the data shows a split at lower frequencies, because there are two different indices of refraction for different magnetic field orientations.

In addition to the frequency dependent delay, one other aspect needs to be considered when interpreting **Figure 3**. At the relatively low frequencies used by FORTE, the bending of the rays adds an additional delay to the signal. This additional delay depends on frequency as $1/f^4$, the angle from the zenith, and the total TEC. In order to estimate the additional path length, either ray-tracing algorithms must be employed to estimate the delay due to the bending of the rays, or the fit to the data in Figure 3 must include the $1/f^4$ dependence.

From a collection of about 20 overpasses the TEC data from the FORTE satellite was estimated from a combined $1/f^2$ and $1/f^4$ fit to the signal delay, only using data down to 40 MHz. The RMSE of the TEC between FORTE and US-TEC was 2.65 TEC units over all the slant paths, equivalent to about 2.0 TEC units. The uncertainty estimates were reasonably consistent with the results from the differential method.
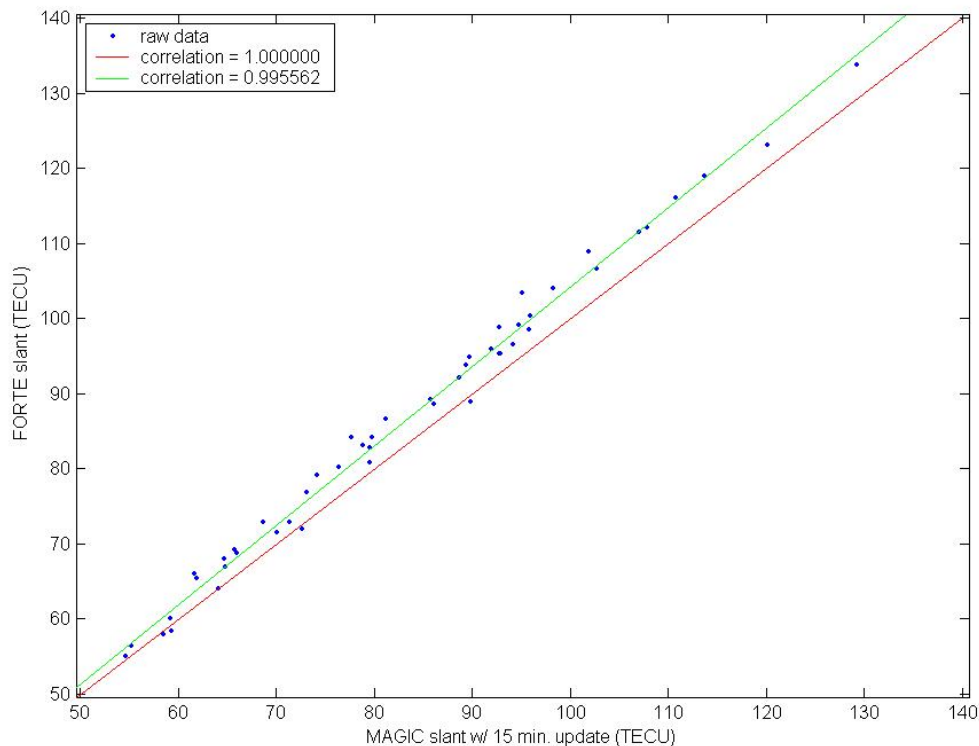

Figure 4: Comparison of slant path TEC from FORTE and US-TEC

The analysis has also been performed using ray-tracing algorithms. **Figure 4** shows a comparison of FORTE and US-TEC for eight overpasses of the satellite. The RMSE for this sample of the dataset is 3.9 TEC units for the slant path, which is equivalent to less than 3 TEC units for the vertical. It is clear from Figure 4 that the uncertainty is not randomly distributed, but there appears to be a bias that is dependent on the absolute magnitude of the TEC. The average bias for the slant path TEC is 3.3 TEC units and standard deviation about the mean is 2.1 TEC units.

There are three possible sources for the difference in FORTE and US-TEC:
1. Uncertainty in the FORTE observations, the fits to the data, or the ray tracing, required to extract the TEC value;
2. Errors in the US-TEC map itself; and
3. Errors introduced in sub-sampling the US-TEC vertical profile.

The latter is a result of the difference in the TEC to the altitude of the FORTE satellite and the total TEC to the GPS satellites. It is necessary to sub-sample the US-TEC inversion to include only the TEC to the satellite altitude. Uncertainties in the vertical profile can lead to the introduction of errors even when the total TEC is precisely known.

4. Conclusion

The analysis of the RMSE for the differential TEC indicates an uncertainty in the slant path TEC of about 2.4 TEC units over the 6-month testing period. This can be compared with 2.65 TEC units for the fits to the FORTE data, and 3.9 TEC units for the estimates using the ray-tracing algorithms. In the first case, the observable is precise but has a possible bias. In the second case, the observable and the sub-sampling of the vertical domain introduce additional uncertainties. The results indicate that the differential TEC RMSE are likely to be valid and to reflect values close to the true uncertainty. The US-TEC uncertainty in the vertical TEC is therefore estimated to be about 2 TEC units during quiet geomagnetic conditions.

The most geomagnetically active day in Table 1 was July 25th with an A_p of 60. The uncertainty rose slightly in US-TEC by about 0.7 TEC units, whereas the IRI reference model increased by substantially more.

Both the differential validation and comparisons of US-TEC with additional FORTE data will proceed in the future.